

# PWM CONTROLLING OF A NEW MULTI DC-DC CONVERTER CIRCUIT

Erol CAN

**Abstract:** The design and development of DC-DC converter circuits are important for increasing and decreasing the direct current energy sources at operating the loads and systems. In this study, a multi DC-DC converter structure is described. The purpose of creating this circuit structure is to create a more effective circuit by offering a different circuit structure. For the proposed DC-DC converter, a circuit structure with five switches is created. This circuit structure is described by mathematical models according to the operation of the four parts PWMs in different time periods. After the mathematical analysis of the circuit structure, the proposed circuit and conventional circuit are operated in the Matlab Simulink. The obtained results are compared. According to the comparisons, the proposed circuit produces a higher output voltage than the traditional one and has a higher performance. Additionally, the circuit is operated for values of different loads using different switching times. Finally, voltages and currents are observed on loads.

**Keywords:** different switching times; multi DC-DC converter; the four parts PWM

## 1 INTRODUCTION

Nowadays, DC-DC converters are needed for many electrical devices used in the industry and social life. Hence, many designs have been focused on DC-DC converter circuits. Some studies [1, 2] show that the simple DC-to-DC converter structures have been used for the dc voltage conversion that a system needs. Some of the converter works have been done to regulate the electrical energy obtained from the solar systems and fuel [3-6]. Some converter studies have addressed the problem of applying a min-type control of a synchronous boost converter using the non-linear control switching surface used in the mixed control equations [7, 8]. It also offers the advantages of the switching surface of the start of the operation of the DC-DC converter and explores its potential use for output voltage regulation [9]. This article, unlike the studies listed in the literature, wishes to create a new DC-DC converter structure and mathematical model against the traditional DC-DC converter structures. The proposed circuit structure with its output voltage multiplexing capability offers superior hardware and a different mathematical model than the conventional converters [10-12]. Since it has a simpler structure than other cascade converters, it contains fewer circuit elements [13-17]. In this circuit structure, five IGBT switches are operated by four different PWMs in different time zones. After running the first stage of the PWM1 and PWM 2 DC-DC converter, PWM 3 and PWM4 manage the second stage cycle to re-increase the output voltage obtained. While the first inductor stores current, the second inductor stores the second inductor current. At the same time, the input source in the first cycle contributes again to the input voltage for the second cycle. At the end of the total cycle, the output voltage for the second stage multiplies the output voltage from the conventional DC-DC converter in the first stage. This circuit structure is described in the second section with a mathematical analysis. In the simulation studies, the circuit is operated after the proposed circuit structure has been created in Matlab Simulink. After the output, volt and coil

currents are monitored by the oscilloscope, and the results are obtained. Then, the results obtained from the conventional DC-DC converters and the proposed circuits are compared. Additionally, the circuit is operated for different loads by using different switching times. According to the results obtained, while the proposed circuit provides the current of different loads from low current values to high current values, it provides a voltage of different loads from high voltage values to low voltage values. The results show that the proposed circuit is superior to other DC-DC converters.

## 2 PROPOSED CONVERTER CIRCUIT STRUCTURE

Fig. 1 shows the circuit structure of the converter. There are S1 to S5 switches on the circuit structure. There is one dc voltage source, two equal inductors which are  $L_1$ ,  $L_2$ ; two diodes which are D1, D2; two equal capacitors which are  $C_1$ ,  $C_2$ . In Fig. 2, there is a four part pulse width modulation that controls these switches.

In the first stage, when the PWM-1 is active on the circuit, the circuit structure will be as in Fig. 3a. While PWM-2 is active on the circuit, the circuit structure is in Fig. 3b.

$V_{dc}$  is  $E \cdot V_{o1}$  is the converter output voltage for the first stage.  $T$  is the time period.  $D$  is the PWM value at the time period. PWM-1 operates the  $V_{dc}$  source and the  $L_1$  inductor on the circuit by means of the S1 and S2 switches. In this case, the current through the inductor reaches its maximum value during the operation of PWM-1. PWM-2 operates the  $V_{dc}$  source and  $L_1$  inductor on the circuit by means of the D1, S1, and S4 switches. In this case, the current through the inductor reaches its minimum value during the operation of the PWM-2. The maximum value of the current at this stage is equal to the negative value of the current as it goes down to the minimum. This gives the output voltage the equation known of the DC-DC converter as in Eq. (1).

$$V_{o1} = \frac{E}{(1-D)} \quad (1)$$

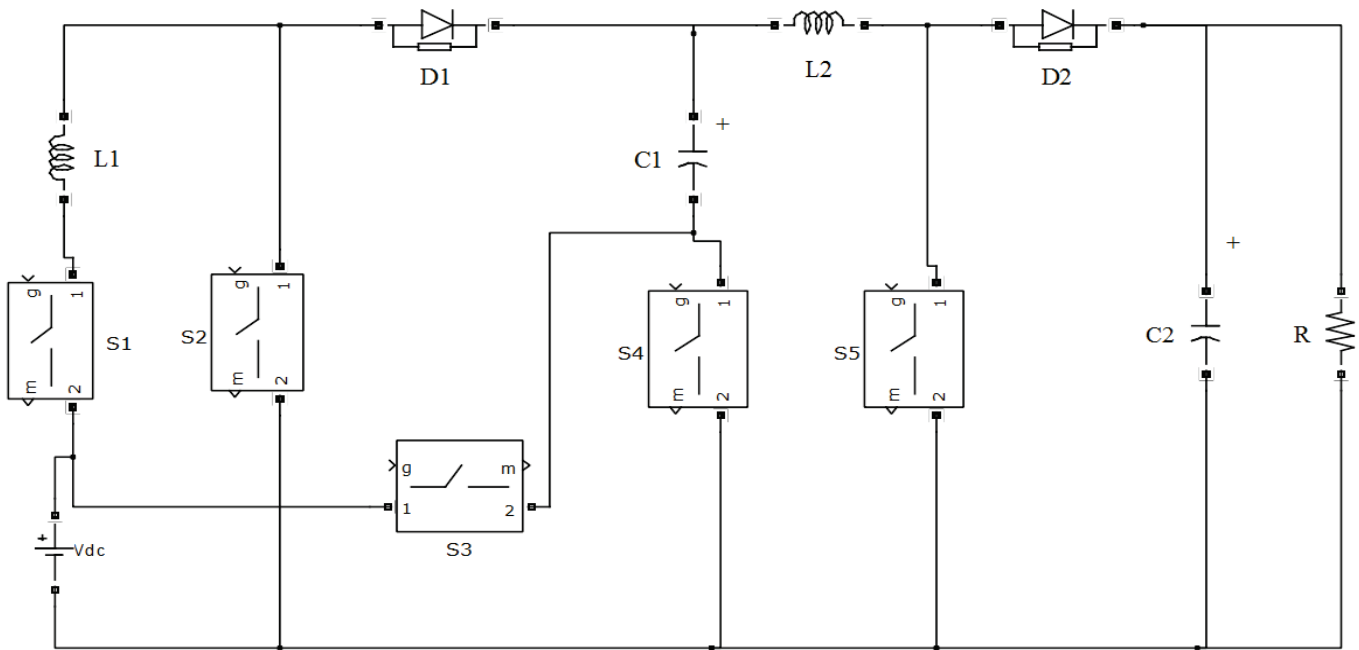


Figure 1 The circuit structure of the converter

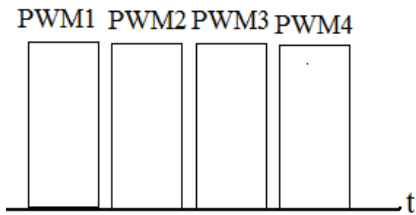


Figure 2 PWMs for the circuit structure of the converter

Since PWM1 and PWM2 constitute half of the total operating time of the PWM, the output voltage is half of the output voltage of the converter operating at full period. Eq. (2) can be written as Eq. (3).

$$V_{o1} = \frac{E}{2(1-D)} \quad (2)$$

In the second stage, when the PWM-3 is active on the circuit, the circuit structure will be as in Fig. 4a. While PWM-4 is active on the circuit, the circuit structure is in Fig. 4b.

$V_{o1}$  is also the converter input voltage at the second stage, while  $V_{o1}$  is the converter output voltage for the first stage. PWM-3 operates the  $V_{dc}$  source,  $L_2$ ,  $C_1$  on the circuit by means of the S3 and S5 of the switches. In this case, the current through the inductor reaches its maximum value during the operation of the PWM-3. The current of the  $L_2$  inductor from the minimum to the maximum value can be written as in Eq. (3).

$$\left( \begin{array}{l} \frac{E}{2(1-D)L_2} = \frac{di_2}{dt} \\ I_{\min} - I_{\max} = \frac{E}{2(1-D)L_2} DT \end{array} \right) \quad (3)$$

PWM-4 operates the  $V_{dc}$  source,  $C_1$ ,  $C_2$  and  $L_2$  on the circuit by means of the D2, S3 switches. In this case, the current through the inductor reaches its minimum value during the operation of PWM-4. The maximum value of the current at this stage is equal to the negative value of the current as it goes down to the minimum. The current of the  $L_2$  inductor from the maximum to the minimum value can be written as in Eq. (4), Eq. (5), and Eq. (6).

$$\frac{E}{2(1-D)} = \frac{di_2}{dt} L_2 + VC_2 \quad (4)$$

$$\frac{E}{2(1-D)L_2} - \frac{VC_2}{L_2} = \frac{di_2}{dt} \quad (5)$$

$$I_{\min} - I_{\max} = \left( \frac{E}{2(1-D)L_2} - \frac{VC_2}{L_2} \right) (1-D)T \quad (6)$$

The negative value of Eq. (6) can be equalized to Eq. (3) and a common arrangement can be made as in Eq. (7) and Eq. (8).

$$DT \frac{E}{2(1-D)L_2} = -\frac{E}{2(1-D)L_2} + \frac{VC_2}{L_2} (1-D)T \quad (7)$$

$$D \frac{E}{2(1-D)L_2} = -\frac{E}{2(1-D)L_2} + \frac{VC_2}{L_2} + D \left( \frac{E}{2(1-D)L_2} - \frac{VC_2}{L_2} \right) \quad (8)$$

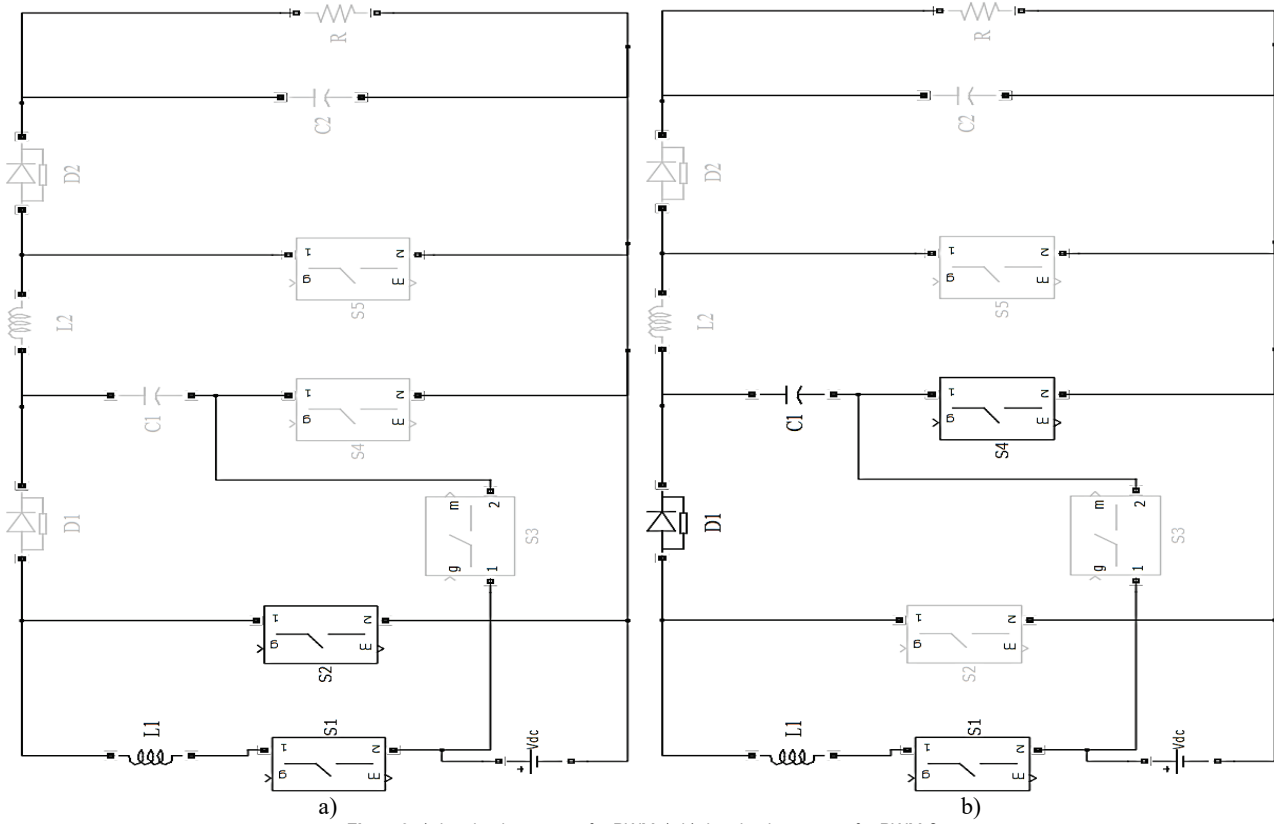


Figure 3 a) the circuit structure for PWM-1, b) the circuit structure for PWM-2

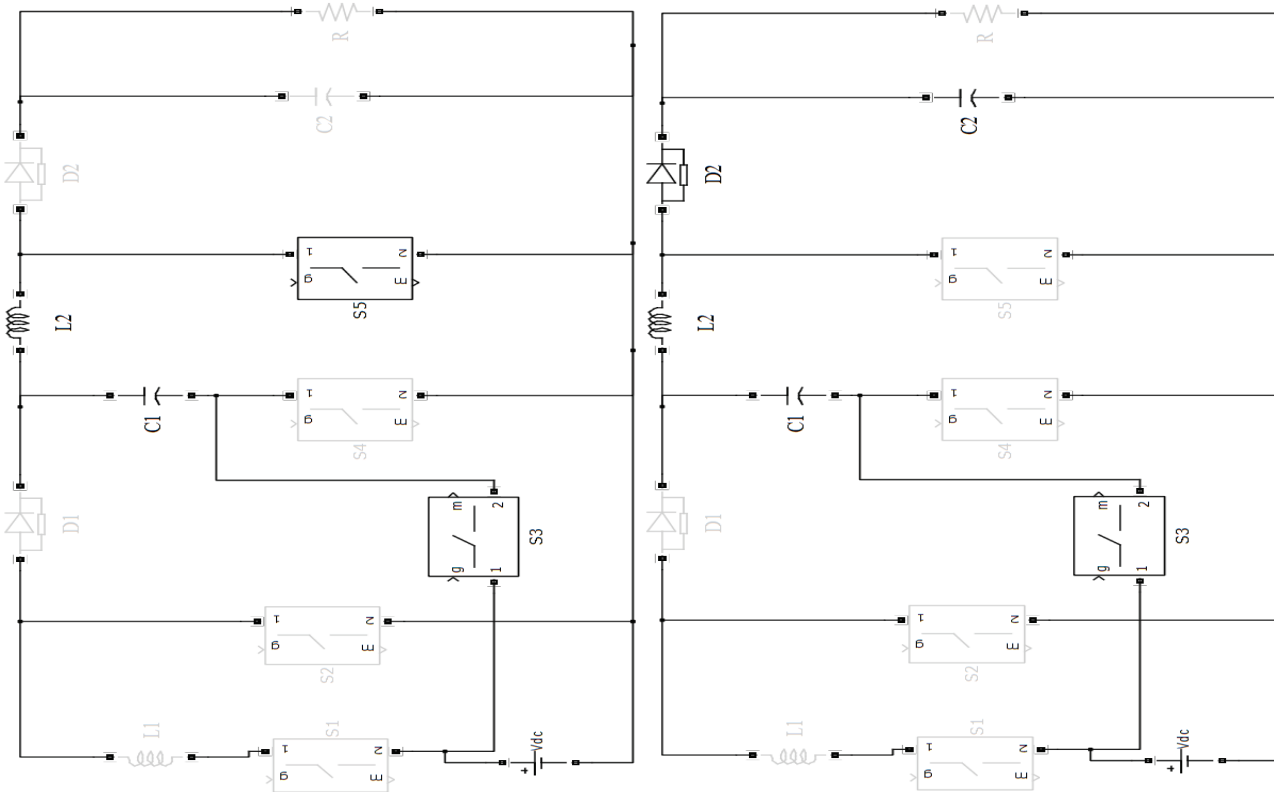


Figure 4 a) the circuit structure for PWM-3, b) the circuit structure for PWM-4

Eq. (8) can be arranged as the equations in Eq. (9), Eq. (10), and Eq. (11). Then, this gives the novel output voltage the equation of the DC-DC converter as in the equations below.

$$\frac{E}{2(1-D)L_2} = -D \frac{VC_2}{L_2} + \frac{VC_2}{L_2} \tag{9}$$

$$\frac{E}{2(1-D)} = (1-D)VC_2 \tag{10}$$

$$\frac{E}{2(1-D)^2} = VC_2 \tag{11}$$

The value of the dividing number in the equation that makes up the  $VC_2$  can be different if the working times of the PWMs were changed. If the number of cycles in the circuit is increased, the number of multiplexes will increase. Hence, the force of  $(1 - D)$  will increase with the increase of the cycle amount.

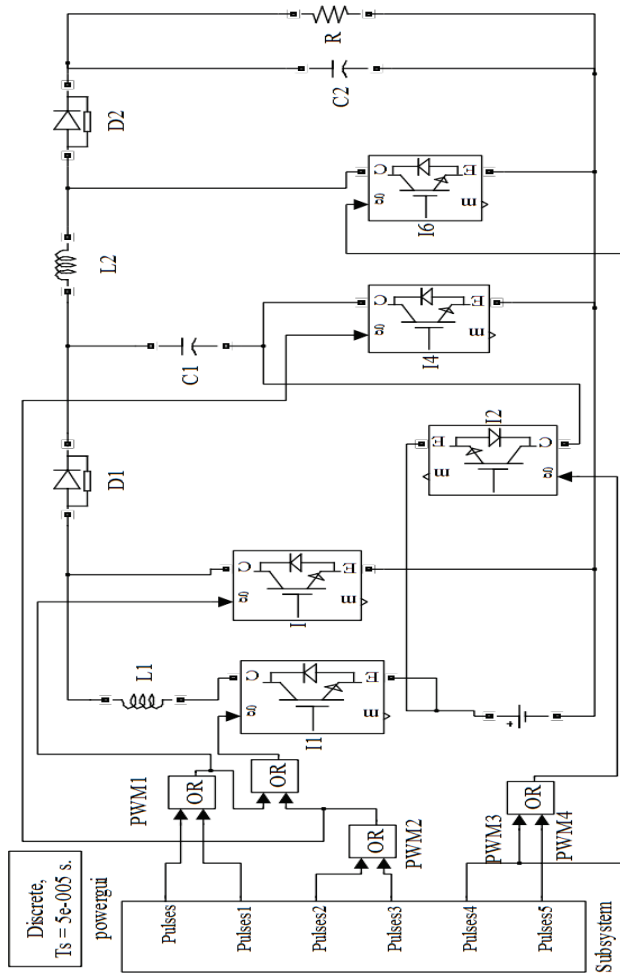


Figure 5 The circuit structure used in the simulation of the multi DC-DC converter

### 3 SIMULATION OF THE MULTIPLE DC-DC CONVERTOR

Fig. 5 shows the circuit structure used in the simulation for the multi DC-DC converter. The multi DC-DC converter has 5 IGBT switches. These switches are operated in 4 different time zones with 4 parts of PWMs that are shown in the Fig. 6.  $L_1 = L_2 = 10$  mH,  $C_1 = C_2 = 10$  mF,  $R = 5$  Ohm. The switching time is 0.01 s.

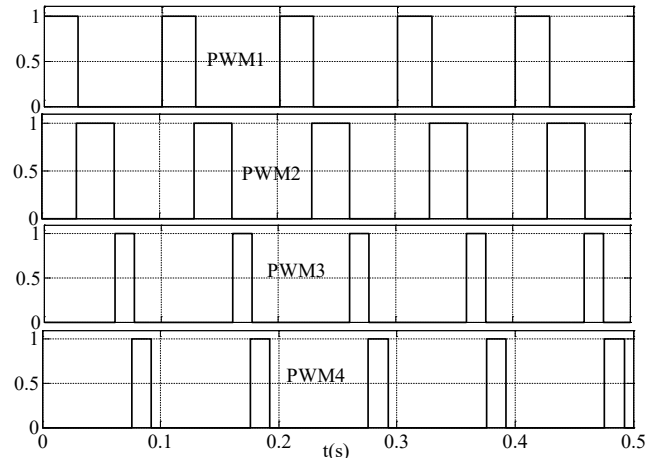


Figure 6 PWMs for the multi DC-DC converter at the simulation

When the proposed circuit is operated in the Matlab Simulink, the current occurring in the  $L_1$  and  $L_2$  inductors for 4 different time periods is as shown in Fig. 7.

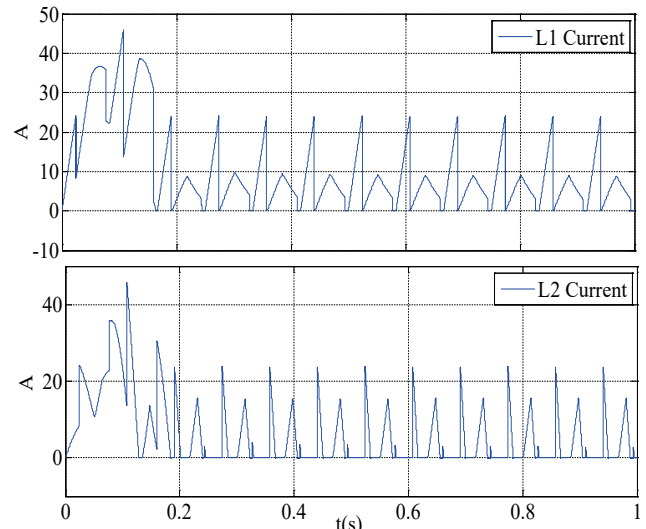


Figure 7 The current occurring in the  $L_1$  and  $L_2$  inductors for 4 different time periods

As seen in Fig. 7, the DC-DC converter structure provides two times the current storage on the coils in order to achieve a higher output voltage than the conventional converters. Current variations are provided in line with the working times of the PWMs on the inductors. The output voltages of conventional converters and multiple converters are shown in Fig. 8 for equal loads.

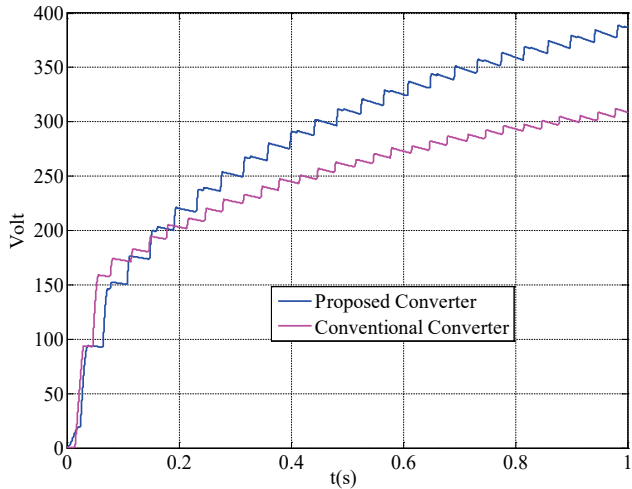


Figure 8 The output voltages of conventional converters and multiple converters for equal loads

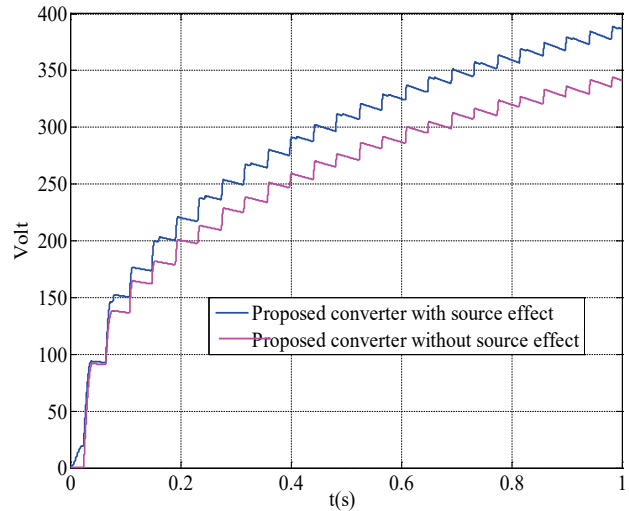


Figure 9 The effect of using the source twice on the output voltages

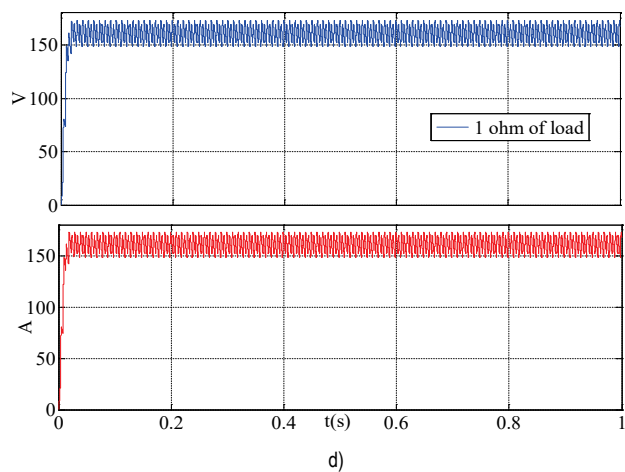
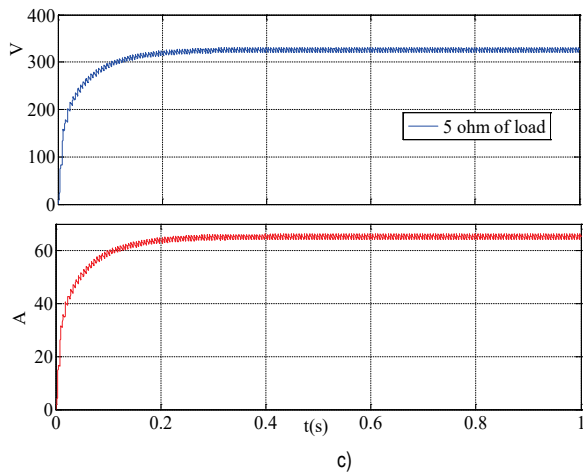
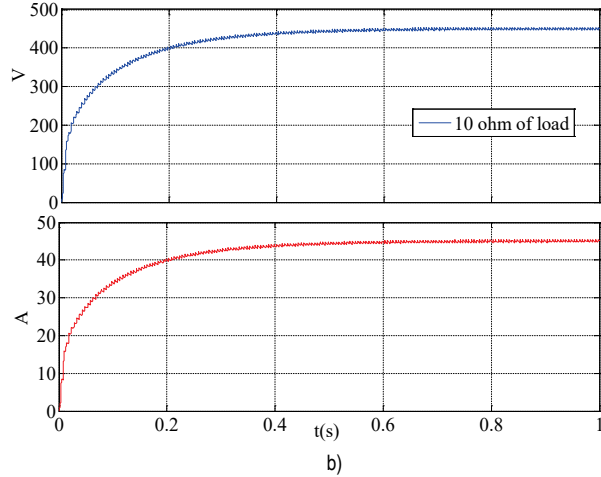
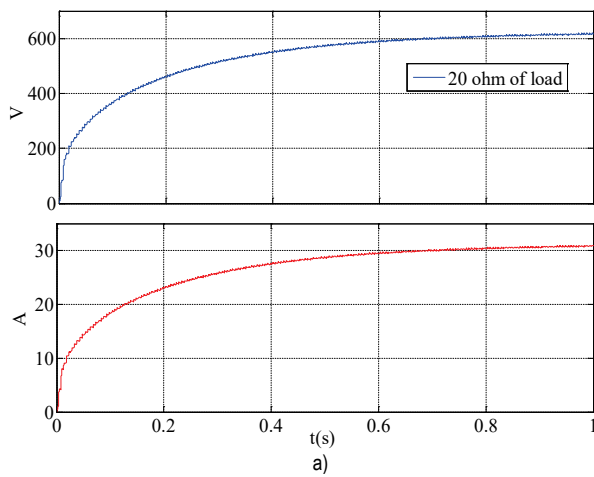


Figure 10 By arranging the switching time to 0.001 sec, the load currents for different load values were obtained

The conventional converter with an input voltage of 50 volts reaches 310 volts at the output voltage, while the multi-DC-DC converter with an input voltage of 50 volts reaches an output voltage of 380 volts. Therefore, the proposed converter structure with a single microcontroller is possible to obtain more output voltage than the conventional converter structure. Another advantage of the multiple DC-DC

converter structure is that it uses a single input voltage source in the first stage, and it is used as the input source in the second multiplexing stage. Therefore, it contributes to a high output voltage. The output voltages, which show the effect of using this source twice, are given in Fig. 9.

In the circuit structure, when the input voltage source is used in the first cycle, the output voltage is 380 V. The output

voltage remains at 340 V when the source is not activated while multiplexing for the second time.

In this study, PWMs in the first cycle have 2 times of the periods according to the second cycle. Therefore, the increases on the output voltage are also percentages. According to a result of the circuit structure operation and results, it provides superiority to conventional converters. Compared to the cascade and the new generation of DC-DC converters, it has less circuit elements and less cost while the proposed converter has a different working order and hardware than them [18-20]. At the same time, it offers a new method of working for a different circuit structure and mathematical models.

By arranging the switching time to 0.001 sec, the switching frequency is increased and the load currents and voltages are shown in Fig. 10 for different load values.

For the simulations from 1ohm of load to 20 ohm of load, the  $L_1$  and  $L_2$  are replaced with 0.1mH in the converter circuit, while  $C_1$  and  $C_2$  are changed to 30 mF. When the circuit is operated for the 20 ohm load, the voltage on the load reaches 600 V and the current value is 30 A. While the circuit is operated for the 10 ohm load, the voltage on the load reaches 450 V and the current value is 45 A. At the 10 ohm load, according to the 20 ohm load, the current value is an increase of 15A, while a decrease of 150 V occurs. While the circuit is operated for the 5 ohm load, the voltage on the load reaches 340 V and the current value is 68 A. At the 5 ohm load, according to the 10 ohm load, the current value is an increase of 23 A, while a decrease of 110 V occurs. When the circuit is operating at the 1 ohm of load, the current and voltage values are 150 A, and 150 V. According to these results, the proposed circuit provides different current and voltage values for different loads.

#### 4 CONCLUSION

This article described the structure of the multi DC-DC converter. The circuit structure of the converter, which has a more advanced structure than the conventional DC-DC converter structure, has been described and simulation studies have been made for this circuit structure. The results obtained from the proposed circuit were compared with the results obtained from the conventional DC-DC converter. While the 50-volt of the dc input voltage was increased to 310 V with the conventional DC-DC converter, the input voltage was increased to 380 volts with the proposed circuit. This was achieved through the current storage by operating in different time segments of two different inductors on the same circuit structure. Additionally, the circuit was operated for different loads using different switching times. When the circuit was operated for the 20 ohm of load, the voltage on the load reached 600 V and the current value was 30 A. While the circuit was operated for the 10 ohm of load, the voltage on the load reached 450 V and the current value was 45 A. At the 10 ohm of load, according to the 20 ohm of load, the current value faced an increase of 15A, while a decrease of 150V occurred. While the circuit was operated for the 5 ohm of load, the voltage on the load reached 340 V and the current value was 68 A. At the 5 ohm of load, according to the 10

ohm of load, the current value faced an increase of 23A while there was a decrease of 110V at the load. When the circuit was operating at the 1 ohm of load, the current and voltage values were 150 A, and 150 V. Thus, the DC-DC converter structure with superior new hardware and a mathematical model has been successfully implemented.

#### 5 REFERENCES

- [1] Sanghavi, B. M., Tejaswini, C., & Venkateshappa, V. (2019). DC/DC boost converter using DSP controller for fuel cell. *Perspectives in Communication, Embedded-systems and Signal-processing-PiCES*, 2(10), 248-251.
- [2] Duan, C. & Wu, D. (2019). Nonlinear Voltage Regulation Algorithm for DC-DC Boost Converter with Finite-Time Convergence. *Journal of Control Science and Engineering*. <https://doi.org/10.1155/2019/6761784>
- [3] Suryadevara, R. & Parsa, L. (2019). Full-Bridge ZCS-Converter-Based High-Gain Modular DC-DC Converter for PV Integration with Medium-Voltage DC Grids. *IEEE Transactions on Energy Conversion*, 34(1), 302-312. <https://doi.org/10.1109/TEC.2018.2878964>
- [4] Chandrasekar, B., Nallaperumal, C., & Dash, S. S. (2019). A Nonisolated Three-Port DC-DC Converter with Continuous Input and Output Currents Based on CUK Topology for PV/Fuel Cell Applications. *Electronics*, 8(2), 214. <https://doi.org/10.3390/electronics8020214>
- [5] Venkatesan, C., Manickam, C., Reddy, M. J. B., Ganesan, S. I., & Chilakapati, N. (2019). Enhanced Power Output from the PV with Low Input Ripple DC-DC Converter. *Electric Power Components and Systems*, 1-12. <https://doi.org/10.1080/15325008.2018.1466214>
- [6] Liu, J., Zheng, Z., Wang, K., & Li, Y. D. (2019). Comparison of boost and LLC converter and active clamp isolated full-bridge boost converter for photovoltaic DC system. *The Journal of Engineering*, 2019(16), 3007-3011. <https://doi.org/10.1049/joe.2018.8507>
- [7] Deaecto, G. S., Geromel, J. C., Garcia, F., & Pomilio, J. (2010). Switched affine systems control design with application to DC-DC converters. *IET Control Theory & Applications*, 4(7), 1201-1210. <https://doi.org/10.1049/iet-cta.2009.0246>
- [8] Albea-Sanchez, C., Garcia, G., & Zaccarian, L. (2015). Hybrid dynamic modeling and control of switched affine systems: application to DC-DC converters. *The 54th Annual Conference on Decision and Control*. IEEE, 2264-2269. <https://doi.org/10.1109/CDC.2015.7402544>
- [9] Sferlazza, A., Martínez-Salamero, L., Sanchez, C. A., Garcia, G., & Alonso, C. (2019). Min-Type Control Strategy of a DC-DC Synchronous Boost Converter. *IEEE Transactions on Industrial Electronics*.
- [10] So, W. C., Tse, C. K., & Lee, Y. S. (1996). Development of a fuzzy logic controller for DC/DC converters: design, computer simulation, and experimental evaluation. *IEEE transactions on power electronics*, 11(1), 24-32. <https://doi.org/10.1109/63.484413>
- [11] Can, E. & Sayan, H. H. (2017). The performance of the DC motor by the PID controlling PWM DC-DC boost converter. *Tehnički glasnik*, 11(4), 182-187.
- [12] Can, E. & Sayan, H.H. (2016). SSPWM three phase inverter design and experimented on unbalanced loads. *Tehnički vjesnik*, 23(5), 1239-1244. <https://doi.org/10.17559/TV-20150730222021>

- [13] Sanjeevikumar, P. & Rajambal, K. (2008). Extra-high-voltage DC-DC boost converters topology with simple control strategy. *Modelling and Simulation in Engineering*, 6. <https://doi.org/10.1155/2008/593042>
- [14] Majeed, Y. E., Ahmad, I., & Habibi, D. (2019). A Multiple-Input Cascaded DC-DC Converter for Very Small Wind Turbines. *IEEE Transactions on Industrial Electronics*, 66(6), 4414-4423. <https://doi.org/10.1109/TIE.2018.2863214>
- [15] Hu, X., Ma, P., Wang, J., Tan, G., & Yao, Z. (2019). A Hybrid Cascaded DC-DC Boost Converter with Ripple Reduction and Large Conversion Ratio. *IEEE Journal of Emerging and Selected Topics in Power Electronics*. <https://doi.org/10.1109/JESTPE.2019.2895673>
- [16] Yu, J., Liu, M., Song, D., Yang, J., & Su, M. (2019). A Soft-Switching Control for Cascaded Buck-Boost Converters without Zero-Crossing Detection. *IEEE Access*, 7, 32522-32536. <https://doi.org/10.1109/ACCESS.2019.2903841>
- [17] Can, E. (2019). The Design and Experimentation of the New Cascaded Dc-Dc Boost Converter for Renewable Energy. *International Journal of Electronics*, 106(9), 1374-1393. <https://doi.org/10.1080/00207217.2019.1591529>
- [18] Lee, S. W. & Do, H. L. (2019). Quadratic Boost DC-DC Converter with High Voltage Gain and Reduced Voltage Stresses. *IEEE Transactions on Power Electronics*, 34(3), 2397-2404. <https://doi.org/10.1109/TPEL.2018.2842051>
- [19] Uno, M. & Shinohara, T. (2019). Module-Integrated Converter Based on Cascaded Quasi-Z-Source Inverter with Differential Power Processing Capability for Photovoltaic Panels Under Partial Shading. *IEEE Transactions on Power Electronics*. <https://doi.org/10.1109/TPEL.2019.2906259>
- [20] Uno, M. & Shinohara, T. (2019). Module-Integrated Converter Based on Cascaded Quasi-Z-Source Inverter with Differential Power Processing Capability for Photovoltaic Panels Under Partial Shading. *IEEE Transactions on Power Electronics*. <https://doi.org/10.1109/TPEL.2019.2906259>

**Author's contacts:**

Dr. Erol CAN, Assistant Professor  
School of Civil Aviation, Erzincan University,  
Aviation Electrical Electronics, 24100 Erzincan, Turkey  
E-mail: can\_e@hotmail.com